Montastraea cavernosa corallite structure demonstrates 'shallow-only' and 'depth-generalist' morphotypes across shallow and mesophotic depth zones in the Gulf of Mexico

Michael S Studivan[1]*, Gillian Milstein[2], Joshua D. Voss[1]

[1] Harbor Branch Oceanographic Institute, Florida Atlantic University, Fort Pierce, FL, USA

[2] Corning School of Ocean Sciences, Maine Maritime Academy, Castine, ME, USA

* Corresponding author

E-mail: studivanms@gmail.com (MSS)

Abstract

This study assessed morphological variation in corallite structure of the depth-generalist coral *Montastraea cavernosa* across shallow and mesophotic coral ecosystems in the Gulf of Mexico (GOM). Among eight corallite metrics examined, corallite diameters were smaller and spacing was greater in mesophotic corals as compared to shallow corals. Additional corallite variation, including greater corallite height of mesophotic samples, were hypothesized to be photoadaptive responses to low light environments. Although comparison of shallow and mesophotic *M. cavernosa* was the initial objective of the study, multivariate analyses revealed two distinct morphotypes able to be identified by the significant variation in corallite spacing with >90% accuracy. A 'shallow-only' morphotype was characterized by larger, more closely-spaced corallites, while a 'depth-generalist' type exhibited smaller, further-spaced corallites. The depth-generalist morphotype comprised the majority of mesophotic *M. cavernosa* colonies sampled from sites in the northwest GOM including the Flower Garden Banks (FGB), Bright Bank, and McGrail Bank. A combination of both morphotypes were found at shallow depths in the FGB. Conversely, in the southeast GOM, the shallow-only morphotype was observed in shallow Dry Tortugas. Mesophotic *M. cavernosa* at Pulley Ridge were comparable to the shallow-only morphotype in terms of corallite spacing but shared morphological similarities with mesophotic corals for other measured characters, likely representing a hybrid morphology. The variable presence of the morphotypes across sites likely indicates a genotypic influence on corallite morphology, as there was a slight, but significant, impact of morphotype on genetic differentiation within the FGB. Patterns of increased algal symbiont (Symbiodiniaceae) density and chlorophyll concentration were retained in the depth-generalist morphotype even at shallow depths, suggesting multiple photoadaptive strategies between morphotypes. Despite the observed

polymorphism in shallow and mesophotic *M. cavernosa*, the implications for these morphological differences in coral physiology and fitness are not fully known, although some evidence suggests skeletal optical properties may influence bleaching resilience.

Introduction

Using morphology as the sole method of species delineation can be confounded in scleractinian corals due to the considerable morphological variation observed within some species [1–6]. Occurrences of homologous morphological characteristics among coral species that are genetically distant from one another suggest further limitations for taxonomy based solely on morphology [7]. In one notable case in the Tropical Western Atlantic (TWA), high levels of skeletal variation observed in the *Orbicella* (previously *Montastraea) annularis* species complex, in conjunction with observed niche partitioning, resulted in the split of the complex into three sister species [8–10]. With additional genotyping efforts, *M. cavernosa* was determined to be the only species within the genus *Montastraea*, while the remaining three species formerly of the *M. annularis* species complex were reassigned to the genus *Orbicella* [5]. In other cases, however, some corals can demonstrate remarkable levels of morphological variation across environments.

Variation in skeletal structure within a species is thought to be the interactive result of environmental stimuli and genotype. There is debate whether genotype contributes more heavily to coral morphology [11], or whether a combination of both genotype and environmental conditions act as simultaneous drivers [9,12,13]. Tests of environmental versus genotypic influence on phenotype through reciprocal transplant experiments have demonstrated that the environment has significant influence on coral morphology, but that genotype may limit the

64 degree of morphological plasticity [14]. Previous studies have also identified a significant
65 interaction between genotype and environmental conditions following transplantation, meaning
66 genetics contributed to variation in polyp morphology differently over a range of environmental
67 conditions [15,16]. Differences in intracolony variation across populations provides further
68 evidence for a genotypic influence on coral morphology [17], given the varying degrees of
69 genotypic diversity observed across reefs at multiple spatial scales [18,19]. The lack of
70 comprehensive genetic markers for most coral species has limited the examination of genotypic
71 influence on morphological variation to manipulative experiments over *in situ* assessments,
72 therefore most previous research focuses instead on describing phenotypic and physiological
73 responses to environmental conditions.

74 Light levels and flow patterns are hypothesized to be the two dominant drivers of coral
75 phenotype [20,21], affecting colony-wide morphologies such as shape and rugosity [22,23]. On a
76 smaller scale, corallite characteristics including corallite area, columella area, and septal length
77 increase in size with higher light levels. This effect has been demonstrated using reciprocal
78 transplants with *O. annularis*, *Favia speciosa*, and *Diploastrea heliopora*, where clonal colonies
79 moved to areas with increased light levels grew larger polyps [12,16]. Conversely, at depth, *O.*
80 *annularis* polyps were smaller and further apart, requiring less tissue and therefore less metabolic
81 support [9,24,25]. Both light and water flow can differ substantially across depth gradients [26–
82 29], indicating the potential for noticeable differences in colony and corallite morphologies.

83 Polyp size and spacing have implications for feeding method and efficiency as well.
84 Increased polyp spacing with depth may also maximize photosynthetic efficiency, as less
85 crowded polyps reduce self-shading of algal symbionts (Symbiodiniaceae) and photosynthetic
86 pigments, thereby increasing the amount of light available to each polyp [15,30,31]. There is an

established positive link between depth and heterotrophic rates in deeper corals due in part to increased nutrient upwelling at depth [32–40], but the relationship between polyp size and heterotrophy is not fully understood [41]. Few studies have identified a link between corallite structure and polyp behavior, suggesting that smaller polyps tend to have diurnal expansion, theoretically increasing feeding time [25,42]. Smaller polyps have also been shown to correlate with a higher ratio of tentacles exposed to food to interpolyp tissue area compared to larger polyps with more tissue area lacking tentacles [43]. Considering that polyps become smaller with depth [9], it is possible that the combination of smaller and further-spaced polyps are an adaptive response to increase both light and food capture at depth.

Currently, there is limited understanding of intraspecific morphological variation across shallow coral reefs and mesophotic coral ecosystems (~30–150 m) [6,26,44], primarily due to a lack of morphological data collected beyond 20 m. Recent studies of *M. cavernosa* in Bermuda have suggested that similar trends as described previously extend into the mesophotic depth zone, as corallites and overall colony sizes were observed to be smaller than at shallow depths [45,46]. The authors suggested that the micromorphological plasticity in this species was the result of photoadaptation and not necessarily selection as there was limited evidence of genetic differentiation between depth zones [47]. Furthermore, it was hypothesized that colony growth rates were lower at mesophotic depths, but that higher abundance of colonies at depth suggest a well-established mesophotic population [45]. While there is a general understanding of environmental characteristics that may influence coral physiology and morphology at mesophotic depths [reviewed in 28,42,43], environmental data regarding downwelling irradiance and zooplankton abundance is unknown for most mesophotic habitats.

The ecology of corals across shallow and mesophotic coral ecosystems is only beginning to be explored. Genetic connectivity of coral populations across depths is contingent on similarities between shallow and mesophotic conspecifics and may be affected by potential morphological lineages within a species [25,42,50]. Therefore, it is important to understand the level of morphological variation within coral populations and to determine whether that variation is reflective of genetic structure and connectivity. It is estimated that 25–40% of scleractinian species in the TWA are considered depth-generalists, some of which are ubiquitous across shallow and mesophotic habitats [35,51]. Depth-generalists present an opportunity to observe phenotypic variation of a species across a wide habitat range, yet within a small vertical scale to minimize any potential interactive effects of reef environments. An assessment of existing functional and physiological differences between shallow and mesophotic conspecifics is necessary to understand the potential for adaptation to different environments. Any potential similarities in coral morphology across depth zones may not only indicate the possibility for morphotypes within species to adapt to different environments, but also reveal the presence of genetic influences on morphological plasticity. Through examination of micromorphological variation in the depth-generalist species *M. cavernosa* across a wide range of geographical locations, we examined whether there exists a significant shift in corallite structure between shallow and mesophotic coral populations. Furthermore, we aimed to address whether evidence of adaptation to low-light environments is represented in known genotypic variation across populations.

Materials and methods

Study sites and sample collection

Morphological variation in *Montastraea cavernosa* was assessed through sampling at shallow and mesophotic sites in the northwest and southeast Gulf of Mexico (NW GOM and SE GOM, respectively). Approximately 180 km off the coast of Galveston, Texas in the NW GOM, the Flower Garden Banks (FGB) include West and East FGB. Residing on salt domes on the continental shelf, both sites are comprised of relatively shallow (17–20 m) coral caps and surrounding mesophotic margin habitats to 40–55 m [52,53]. East of the FGB, additional banks along the shelf margin provide habitat for mesophotic-only reefs (50–75 m) including Bright and McGrail Banks. *Montastraea cavernosa* is ubiquitous in the region and one of the most abundant scleractinian species at each site sampled in the NW GOM [54–56]. In the SE GOM, Pulley Ridge occupies the continental shelf margin southwest of Florida and is currently the deepest known hermatypic coral reef in US territory [57]. Coral diversity on the ridge and surrounding reef habitat is low, but *M. cavernosa* are present in the mesophotic coral communities found between 65–75 m [58,59]. The closest shallow coral habitat is found ~66 km east in the Dry Tortugas, with *M. cavernosa* populations between 1–35 m [60].

In total, 212 *M. cavernosa* samples were collected across six sites in the GOM during expeditions in 2014–2016. Vertically-contiguous reef habitats exist within the FGB, allowing direct comparison of morphology between shallow and mesophotic depth zones within sites. For these collections, the coral caps of West and East FGB (WFGB and EFGB, respectively) were sources of relatively shallow samples collected at 20 m. Along the bank margins, mesophotic samples were collected at 45 m. Fifty-nine coral fragments were collected from West FGB (shallow, n=30; mesophotic, n=29) and 59 fragments were collected from East FGB (shallow,

152 n=37; mesophotic, n=22). Mesophotic samples were collected from the 50 m caps at Bright Bank
153 (BRT, n=19) and McGrail Bank (MCG, n=26). Twenty five fragments were collected at the
154 mesophotic-only Pulley Ridge (PRG) at 65 m and 24 fragments were collected at the nearby
155 shallow-only Dry Tortugas (DRT) at 29 m. Coral fragments approximately 15–25 cm^2 in area
156 were collected from the margins of *M. cavernosa* colonies by SCUBA divers with a hammer and
157 chisel or a remotely-operated vehicle (ROV) with a five-function manipulator and suction
158 sampler. Subsamples designated for morphometric analyses required at least five undamaged
159 polyps and intact neighboring polyps; additionally all polyps measured were at least one row of
160 polyps away from colony margins [17]. Fragments were processed with a dental water pick
161 (Waterpik Water Flosser) to remove coral tissue and subsequently bleached in a 10% sodium
162 hypochlorite solution to remove any remaining connective tissue or surface skeletal color.

163 Morphological characters

164 Thirteen morphometric characters were identified from previous studies of morphological
165 variation in *M. cavernosa* [2,17,21,42]. These metrics were quantified for a subset of available
166 samples to determine if any characters could be eliminated while still maximizing morphological
167 variation captured. Five of the characters lacked significant variation across samples, had strong
168 correlations with other metrics, or included inherent variability that may have compromised the
169 ability to recognize variation across samples (*e.g.* costal structures were frequently eroded in
170 between corallites and therefore produced inconsistent length measurements across corallites; S1
171 and S2 Tables). Those excluded from further analyses were: thickness of the first cycle septa
172 (T1S), length of the first cycle costa (L1C), thickness of the fourth cycle septa (T4S), length of
173 the fourth cycle costa (L4C), and thickness of the fourth cycle costa (T4C). The remaining eight
174 morphometric characters used in the analyses presented here included: corallite diameter (CD),

175 columella width (CW), length of the first cycle septa (L1S), thickness of the first cycle costa
176 (T1C), length of the fourth cycle septa (L4S), theca height (TH), corallite height (CH), and
177 corallite spacing (CS) (Table 1, Fig 1). Characters CH and TH were measured to the nearest 0.01
178 mm using dental calipers (ProDent USA). Scaled photographs were taken by a Canon G12
179 camera with a 6.1–30.5 mm lens (~10–20 mm focal length) with the target corallite centered to
180 minimize edge distortion and ensuring the corallite surface was perpendicular to the lens angle
181 using a bubble level. The remaining metrics were measured using the scaled photographs in
182 ImageJ [61,62].
183
184 **Table 1. Corallite morphological characters.**

Metric	Abbrev.	Description
Corallite diameter	CD	Linear measure between corallite cavity margins
Columella width	CW	Linear measure across columella
Length 1st cycle septa	L1S	Linear measure of first cycle septa length
Thickness 1st cycle costa	T1C	Linear measure of first cycle costa thickness
Length 4th cycle septa	L4S	Linear measure of fourth cycle septa length
Theca height	TH	Linear measure between columella floor and theca
Corallite height	CH	Linear measure between corallite base and peak
Corallite spacing	CS	Linear measures between corallite and all neighbors

185 Morphometric characters compiled from previous assessments of *Montastraea cavernosa*
186 skeletal variation [2,17,21,42].
187
188 **Fig 1. Corallite morphological characters photo panel.** A: Five of the eight morphometric
189 characters chosen for this study superimposed over a *Montastraea cavernosa* corallite. Not
190 pictured: CH (corallite height), TH (theca height), and CS (corallite spacing). B: Typical corallite

appearance for ‘shallow-only’ morphotype. C: Typical corallite appearance for ‘depth-generalist’ morphotype. Panels B and C were photographed at equal scales.

Statistical analyses

Means and standard deviations of each morphological character were calculated for coral samples and duplicate statistical analyses were conducted on both datasets to assess intercolony and intracolony morphological variation, respectively. Coral sample data were analyzed using non-parametric tests due to violations of normality assumptions that could not be corrected via transformation. First, each morphological character was analyzed for significant variation across a single-factor combination of site and depth zone using Kruskal-Wallis tests. Pairwise comparisons were conducted using Dunn’s tests and *p* values were false discovery rate (FDR)-corrected in the R package *FSA* [63]. Two-way permutational multivariate analyses of variance (PERMANOVAs) tested the interactive effects of site (WFGB, EFGB, BRT, MCG, PRG, DRT) and depth zone (mesophotic, shallow) on overall corallite morphology, including pairwise comparisons within factors. Additional pairwise comparisons were conducted for West and East FGB samples as an assessment of morphological variation across depth zones within the Flower Garden Banks. Test conditions for two-way PERMANOVAs utilized Euclidean distance, Type III SS, permutation of residuals under a reduced model, and 9999 model permutations in Primer v7 [64,65]. Subsequently similarity percentage tests (SIMPER) determined which morphometric characters contributed most strongly to differences observed among site and depth factor groups. SIMPER parameters utilized Euclidean distance and an 80% contribution cutoff.

Corallite morphological variation was visualized with principal coordinates analysis (PCoA). Two potential morphotypes were identified across all sites using sample groupings in

214 the PCoA. Clustering patterns from the PCoA were tested for the presence of two morphotypes
215 using a *k*-means clustering test (kRCLUSTER) with *k*=2. Frequency distributions were
216 visualized for the six most variable characters across depth (CD, CW, CS, TH, CH, and L1S) to
217 attempt to identify a threshold measurement that would allow a quantitative determination of
218 morphotype from a single character. Morphotype assignments from the *k*-means clustering tests
219 were compared to assignments from the CS metric to determine assignment accuracy. To assess
220 which morphological characters differed between morphotypes while controlling for variation in
221 environmental conditions across depth, a subset dataset was created using samples from the
222 shallow caps (20 m) at West and East FGB. Additionally, corresponding algal symbiont
223 (Symbiodiniaceae) density, areal chlorophylls *a* and *c2*, cellular chlorophylls *a* and *c2*, and
224 chlorophyll *a*:*c2* ratio data from a recent study of the same coral colonies [66,67] were added to
225 the analyses. Symbiont and chlorophyll data were collected as described in Polinski and Voss
226 [66]. This reduced dataset was tested for significant differences between 'depth-generalist'
227 (n=20) and 'shallow-only' (n=46) morphotypes using Mann-Whitney U tests with the R package
228 *ggpubr* [68]. Next, separate one-way PERMANOVA and SIMPER tests were conducted to
229 determine if overall corallite morphology and overall symbiont/chlorophyll parameters were
230 different between morphotypes sampled from the same depth zone.
231 Morphotype assignments for samples from West and East FGB were also matched to
232 genotypes generated from the same samples to identify any relationship between corallite
233 morphology and genetic structure [69]. Based on previous assessments of low genetic
234 differentiation among depth zones within and between West and East FGB, samples were
235 combined to form two populations based on morphotype assignments. Samples missing
236 sufficient microsatellite marker coverage were removed from the analyses. Multi-locus

genotypes were scored and normality assumptions were checked as described in Studivan and Voss [69] and assessment of population structure (with depth-generalist: n=70, shallow-only: n=35) was conducted with an analysis of molecular variance (AMOVA) using fixation index (F_{ST}) in GenAlEx 6.5 [70,71] and with genetic structure analysis in Structure 2.3.4 and Structure Harvester [72–74].

Results

Corallite variation

Mean measurements of the eight corallite characters at the six GOM sites are presented in Table 2. Corals collected from shallow depths had larger, more tightly-spaced corallites than their mesophotic counterparts. Furthermore, shallow corallites were flatter compared to the surrounding skeleton but had deeper thecal depressions than mesophotic corallites (Kruskal-Wallis: CD, p=3.5e^{-8}; CW, p=1.4e^{-13}; L1S, p=2.0e^{-16}; L4S, p=2.0e^{-16}; T1C, p=2.0e^{-16}; TH, p=1.3e^{-12}; CH, p=2.0e^{-16}; CS, p=2.0e^{-16}; Table 2, Fig 2, S3 Table, S1 Fig). The two-way PERMANOVA of all samples revealed both site (Pseudo-$F_{5, 204}$=14.99, p=0.0001) and depth zone (Pseudo-$F_{1, 204}$=70.12, p=0.0001) as significant factors for corallite morphology across all metrics, while the interaction between site and depth zone was not significant (Pseudo-$F_{1, 204}$=2.55, p=0.066). Pairwise PERMANOVA comparisons among sites within depth zones identified significant morphological variation primarily between both Pulley Ridge and Dry Tortugas compared to all other sites (Table 3). Pairwise comparisons between depths at West and East FGB showed a significant effect of depth zone on overall corallite morphology (WFGB: t=5.13, p=0.0001; EFGB: t=5.98, p=0.0001). Replicated statistical tests using standard deviation instead of sample means corroborated the same trends (site: Pseudo-$F_{5, 204}$=5.05, p=0.0001;

depth: Pseudo-$F_{1, 204}$=18.94, p=0.0001; interaction: Pseudo-$F_{1, 204}$=0.29, p=0.89; S4 Table), indicating that intracolony variation was likely accounted in the sampling and measurement design. SIMPER analyses revealed that corallite variation between shallow and mesophotic depths across all sites were primarily attributed to CS (73.15%) and CD (11.61%).

Table 2. Corallite sample means.

Site	Depth Zone	Sampling Depth (m)	Sample Size (n)	Size in mm ± SEM							
				CD	CW	L1S	L4S	T1C	TH	CH	CS
West Flower Garden Bank	mesophotic	45	29	5.76 ± 0.09	2.32 ± 0.05	1.64 ± 0.03	0.51 ± 0.02	0.32 ± 0.01	2.06 ± 0.05	3.10 ± 0.11	10.06 ± 0.25
	shallow	20	30	6.79 ± 0.18	2.88 ± 0.09	1.22 ± 0.07	0.39 ± 0.02	0.24 ± 0.01	2.60 ± 0.07	2.75 ± 0.13	7.59 ± 0.36
East Flower Garden Bank	mesophotic	45	22	6.02 ± 0.12	2.53 ± 0.06	1.81 ± 0.05	0.62 ± 0.03	0.34 ± 0.01	2.20 ± 0.07	2.87 ± 0.09	10.49 ± 0.22
	shallow	20	37	6.22 ± 0.18	2.77 ± 0.08	1.18 ± 0.04	0.43 ± 0.01	0.28 ± 0.01	2.68 ± 0.11	2.24 ± 0.06	7.42 ± 0.28
Bright Bank	mesophotic	50	19	5.60 ± 0.17	2.38 ± 0.08	1.53 ± 0.06	0.49 ± 0.02	0.33 ± 0.01	2.07 ± 0.08	3.19 ± 0.13	9.68 ± 0.31
McGrail Bank	mesophotic	50	26	5.70 ± 0.12	2.27 ± 0.04	1.66 ± 0.05	0.51 ± 0.02	0.32 ± 0.01	2.28 ± 0.03	2.82 ± 0.13	9.71 ± 0.24
Pulley Ridge	mesophotic	65	25	4.99 ± 0.20	2.24 ± 0.08	0.84 ± 0.02	0.29 ± 0.01	0.18 ± 0.01	2.50 ± 0.12	1.41 ± 0.11	7.23 ± 0.20
Dry Tortugas	shallow	29	24	6.41 ± 0.18	3.04 ± 0.06	0.94 ± 0.03	0.35 ± 0.01	0.23 ± 0.01	3.05 ± 0.11	1.75 ± 0.07	6.73 ± 0.22

Mean ± standard error of the mean (SEM) of eight corallite morphometrics across six sites and two depth zones in the Gulf of Mexico.

Fig 2. Corallite sample means. Boxplots with sample overlays for corallite spacing (CS), corallite diameter (CD), corallite height (CH), and theca height (TH) across six sites and two depth zones in the Gulf of Mexico. Overall p values represent Kruskal-Wallis tests across sites and depth zones for each metric and different letters denote significant differences (p<0.05) between pairwise comparisons of sites and depth zones generated by Dunn's tests.

274 **Table 3. PERMANOVA results**

Test	Comparison	Test Statistic	*p* value
Overall	Site	14.99	0.0001
	Depth	70.12	0.0001
	Site – Depth interaction	2.55	ns
Within shallow	EFGB – DRT	1.89	0.025
	EFGB – WFGB	1.37	ns
	DRT – WFGB	2.51	0.003
Within mesophotic	BRT – EFGB	2.07	0.021
	BRT – MCG	0.91	ns
	BRT – PRG	6.01	0.0001
	BRT – WFGB	0.86	ns
	EFGB – MCG	2.03	0.030
	EFGB – PRG	8.34	0.0001
	EFGB – WFGB	1.48	ns
	MCG – PRG	6.52	0.0001
	MCG – WFGB	1.13	ns
	PRG – WFGB	7.62	0.0001
Within WFGB	shallow – mesophotic	5.13	0.0001
Within EFGB	shallow – mesophotic	5.98	0.0001

275 Test results for permutational multivariate analysis of variance (PERMANOVA, Overall) and
276 pairwise comparisons across sites within depth zones and across depth zones within sites.
277 Insignificant pairwise comparisons denoted as ns.

278

279 Principal coordinates analysis clustered samples into two groups (Fig 3). One group
280 consisted of the majority of samples from Bright and McGrail Banks, while a second group
281 consisted primarily of Dry Tortugas samples. The split between morphotypes did not lie between
282 shallow and mesophotic samples, however. Corals from West and East FGB were found in both
283 sample groupings, identifying a dichotomy in overall corallite morphology. A subset of samples

collected on the shallow caps at both FGB sites had more similar corallite structure to mesophotic samples than to the remaining shallow samples. Pulley Ridge samples appeared to share some morphological characteristics of both morphotypes, indicated by sample overlap between both sample clusters in the PCoA (Fig 3). Despite sharing smaller corallite characteristics typical of other mesophotic corals (Fig 2), the Pulley Ridge colonies demonstrated corallite spacing consistent with the morphotype observed most common at shallow depths at both FGB sites and Dry Tortugas. With the exception of Pulley Ridge, the majority of mesophotic corals appeared to be a single morphotype (mesophotic West and East FGB, Bright Bank, and McGrail Bank), while shallow corals were split between both morphotypes.

Fig 3. Principal coordinates analysis of all sites. Principal coordinates analysis (PCoA) plot of corallite morphology across six sites in the Gulf of Mexico, explaining 88.5% of the total variation (PCo 1: 69.2%, PCo 2: 19.3%). Degree of difference among samples represented by Euclidean distance between sample points. Color and shape of each point corresponds to site and depth zone.

Morphotype assignment

Frequency distributions of metrics CD, CW, CS, TH, CH, and L1S revealed relatively unimodal distributions for most metrics except for CS and L1S. The bimodal distribution observed in CS across all samples were indicative of two morphotypes split between 8.2–8.6 mm (Fig 4). All samples were sorted by corallite spacing and assigned a morphotype where CS>8.4 mm was considered ‘depth-generalist’ and CS<8.4 mm was considered ‘shallow-only.’ Morphotype assignments using the CS method were found to have a correct assignment rate of

93.87% when compared to assignments from the *k*-means clustering method (Fig 5; kRCLUSTER: R=0.746, 13 incorrect out of 212 assignments). Morphotype assignments from the *k*-means clustering method were used to create subset datasets of samples collected on the shallow caps at West and East FGB in order to test whether the two morphotypes had significantly different corallite structures in the same environment. The differences among morphotypes were not solely attributed to morphological variation due to depth. The depth-generalist morphotype found at 20 m demonstrated increased corallite spacing and reduced corallite diameter, meaning there were fewer and smaller corallites per unit area as compared to the shallow-only morphotype. Despite having smaller corallites, the depth-generalist morphotype had taller corallites over the surrounding skeleton and notably larger septal lengths (Mann-Whitney U: CS, p=1.6e^{-10}; CD, p=0.0056; CH, p=9.1e^{-5}; L1S, p=5.6e^{-10}; CW, p=9.2e^{-4}; T1C, p=1.3e^{-8}; TH, p=0.86; L4S, p=1.0e^{-5}; Table 4, Fig 6, S2 Fig). A single factor PERMANOVA using morphotype assignment identified a significant difference between depth-generalist and shallow-only morphotypes (Pseudo-$F_{1, 65}$=62.73, p=0.0001). For the SIMPER analysis of morphotypes, CS (70.93%) and CD (13.74%) were the most influential metrics. Mann-Whitney U tests also indicated that symbiont density, areal chlorophylls *a* and *c2*, and cellular chlorophylls *a* and *c2* were significantly higher in the depth-generalist morphotype compared to the shallow-only morphotype (Symbiont Density, p=0.0028; Chl *a*:*c2*, p=0.071; Areal Chl *a*, p=1.7e^{-8}; Areal Chl *c2*, p=7.2e^{-8}; Cellular Chl *a*, p=5.4e^{-5}; Cellular Chl *c2*, p=0.0051; Table 4, Fig 7), despite being found in the same light regime and with similar *Symbiodinium* community assemblages [66]. The single factor PERMANOVA identified a multivariate difference between depth-generalist and shallow-only morphotypes across symbiont and chlorophyll metrics

329 (Pseudo-$F_{1, 65}$=11.329, p=0.0016), and the SIMPER attributed 100% of the contribution to
330 symbiont density.
331
332 **Fig 4. Size distributions of dominant characters.** Frequency distributions for the six
333 morphological metrics representing the majority of corallite variation across depth, including:
334 corallite diameter (CD), columella width (CW), corallite spacing (CS), theca height (TH),
335 corallite height (CH), and length of first cycle septa (L1S). The size threshold of CS (8.40 mm) is
336 represented in the orange vertical line, denoting two morphotypes distinguished primarily by
337 differences in corallite spacing. L1S also had a split distribution but had a less obvious threshold
338 (1.15 mm).
339
340 **Fig 5. Comparison of morphotype assignment methods.** Principal coordinates analysis
341 (PCoA) of corallite morphology across six sites in the Gulf of Mexico, with color overlays
342 corresponding to morphotypes. Morphotype assignments were made using a *k*-means cluster test
343 (left; kRCLUSTER: R=0.746) and by the threshold in corallite spacing (CS) measurements at
344 8.40 mm (right). Assignments using the CS method had a correct assignment rate of 93.87%
345 when compared to assignments from the *k*-means clustering method (13 incorrect out of 212
346 assignments, shown in gray).

Table 4. Morphotype sample means

Morphotype	Sample Size (n)	Size in mm ± SEM								Areal Chl (ug cm^{-2} ± SEM)		Cellular Chl (pg cm^{-2} ± SEM)		Chl *a*:c_2
		CD	CW	L1S	L4S	T1C	TH	CH	CS	chl *a*	chl c_2	chl *a*	chl c_2	
depth-generalist	20	5.85 ± 0.13	2.48 ± 0.06	1.59 ± 0.05	0.49 ± 0.02	0.34 ± 0.01	2.74 ± 0.18	2.82 ± 0.11	9.81 ± 0.20	11.13 ± 0.62	4.35 ± 0.44	7.05 ± 0.62	2.75 ± 0.31	2.71 ± 0.10
shallow-only	46	6.75 ± 0.17	2.97 ± 0.07	1.01 ± 0.02	0.38 ± 0.01	0.23 ± 0.01	2.60 ± 0.06	2.30 ± 0.08	6.42 ± 0.13	6.42 ± 0.20	2.45 ± 0.08	4.86 ± 0.16	1.85 ± 0.06	2.64 ± 0.04

Mean ± standard error of the mean (SEM) of eight measured corallite morphometrics and symbiont density across depth-generalist and shallow-only morphotypes from within the shallow depth zone of West and East Flower Garden Banks.

Fig 6. Morphotype sample means. Boxplots with sample overlays for corallite spacing (CS), corallite diameter (CD), corallite height (CH), and length of first cycle septa (L1S) across depth-generalist (n=20) and shallow-only (n=46) morphotypes sampled within shallow depth zone of West and East FGB. Overall *p* values represent Mann-Whitney U tests between morphotype for each metric.

Fig 7. Morphotype symbiont and chlorophyll means. Boxplots with sample overlays for symbiont density, chlorophyll *a*:*c2*, areal chlorophyll *a*, areal chlorophyll *c2*, cellular chlorophyll *a*, and cellular chlorophyll *c2* across depth-generalist (n=20) and shallow (n=46) morphotypes. Overall *p* values represent Mann-Whitney U tests between morphotype for each metric.

Within the samples from West and East FGB, comparison of population structure using morphotype as a factor revealed that corallite variation had a weak relationship to genetic variation. The fixation index (F_{ST}), which represents the level of genetic differentiation between

365 populations, was low but demonstrated significant genetic structure between depth-generalist and
366 shallow-only morphotypes at both FGB sites (AMOVA: F_{ST}=0.007, *p*=0.008). A second
367 AMOVA using morphotype assignments according to the CS method also demonstrated
368 significant genetic structure (AMOVA: F_{ST}=0.007, *p*=0.005). However, structure analysis using
369 both assignment methods indicated that there was one genetic cluster (K=1, panmixia) found at
370 both FGB sites (S5 Table, S3 Fig), which is reflective of the results of a larger genotypic
371 examination of coral populations in the NW GOM [69].
372

373 # Discussion

374 ## Variation among shallow and mesophotic *M. cavernosa*

375 Previous studies have observed that corallite diameter decreases and corallite spacing
376 increases with diminishing light in some scleractinian species [2,6,9,12,17,24]. This study
377 extends this trend to mesophotic depths with *M. cavernosa* [see also 69], as mesophotic corallites
378 were smaller and further apart than their shallow counterparts. Mesophotic corallites were also
379 taller (corallite height), but internally shallower (theca height) than shallow corallites (Fig 2).
380 The morphological variation across depth zones suggests two possible physiological responses to
381 environmental conditions at mesophotic depths: (1) maximization of tissue area for light capture
382 while minimizing self-shading and metabolic costs [15,25,30], and (2) maximization of tentacle
383 area exposed for food capture [43]. While colonies examined in this study were not observed for
384 polyp extension or feeding behavior, earlier studies with *M. cavernosa* hypothesized that smaller
385 corallites may also correspond with increased polyp expansion, although the tradeoffs between
386 photosynthetic and heterotrophic yields are not well understood [25,41]. Quantification of algal
387 symbiont density and chlorophyll concentration in these same colonies corroborated that

388 mesophotic corals appear photoadapted to low light environments [66,67]. Mesophotic *M.*
389 *cavernosa* from the NW GOM (Flower Garden Banks) and the SE GOM (Pulley Ridge)
390 contained more symbionts and chlorophylls *a* and *c2* than their shallow conspecifics from the
391 Flower Garden Banks and Dry Tortugas, respectively.

392 While increased pigmentation and symbiont densities are common photoadaptive
393 responses to lower-light environments [24,33,75,76], they are suspected to also reduce light
394 penetration to deeper coral tissue levels due to greater optical thickness via self-shading [24].
395 Furthermore, a recent study identified photoconvertible red fluorescent proteins that transform
396 poorly-absorbed blue-green light to orange-red wavelengths for increased light absorption by
397 symbionts, which were found more commonly in mesophotic corals [77]. However, while these
398 strategies may maximize light absorption, they likely result in lower tissue penetration. Corals in
399 light-limited environments such as mesophotic reefs may mitigate the negative effects of
400 photoadaptation with enhanced light scattering from skeletal structures [33,78]. Flat surfaces,
401 such as flattened mesophotic skeletons, can increase light scattering threefold within tissues, with
402 additional enhancement caused by concave surfaces in the interior of corallites and by complex
403 structures such as septa [79–82]. This study identified an increase in mesophotic septal length
404 [see also 2] and corallite height (Fig 2), which may provide increased light scattering at depth. It
405 is likely that a tradeoff exists between overall shallow and mesophotic morphologies, given
406 multiple responses at the symbiotic and skeletal levels, although their effect on coral physiology
407 and intraspecies competition is not well known at this time.

408 Identification of 'depth-generalist' and 'shallow-only' morphotypes

409 Investigation of corallite variation and feeding behavior within *M. cavernosa* has led to
410 one theory of potential cryptic speciation through the identification of morphotypes within the

species [25]. A diurnal morphotype had smaller but continuously open polyps, while a nocturnal morphotype was characterized by larger polyps that were expanded only at night. There were also significant differences in algal symbiont density and colony respiration between the two morphotypes, where larger polyps allowed greater photosynthetic yields but subsequently higher respiration rates. Currently, there is little molecular or reproductive evidence to support the claim of cryptic speciation among the morphotypes [50,83], but surveys along a depth gradient in Puerto Rico uncovered different vertical distributions for the morphotypes. The majority of shallow (6 m) colonies were of the smaller diurnal morphotype, while 60% of the deeper (20 m) colonies were the larger nocturnal morphotype, and the author proposed that morphological variation was due to different environmental conditions across depths and tradeoffs between photosynthesis and feeding rates [42]. It is important to note, however, that a comparable study observed both morphotypes with no clear pattern across depths in Belize, implying that phenotypic plasticity in response to environmental conditions is not the sole factor affecting corallite phenotype [50].

Furthermore, this study identified distinct 'depth-generalist' and 'shallow-only' morphotypes within *M. cavernosa* at six sites examined across the GOM (Fig 3). Differences in overall corallite morphologies were mainly attributed to increased corallite spacing in the depth-generalist type (Fig 1), but there were also significant differences in corallite diameter, corallite and thecal height, and septal length. The depth-generalist morphotype was characterized by smaller and more widely-spaced corallites that were taller over the surrounding skeleton (Fig 6). We observed that the variation in corallite spacing alone was enough to predict the correct morphotype assignment with a relatively high level of accuracy (93.87%) compared to a cluster analysis of morphological variation across all eight characters (Fig 5). This is of potential interest

434 for rapid, non-consumptive morphotype identification of *M. cavernosa* colonies *in situ*, perhaps
435 allowing targeted sampling of morphotypes for comparative genotyping analyses. Assignment
436 accuracy using the CS method was also consistently high across large spatial scales in the GOM
437 (~1,000 km), suggesting the possibility of widespread presence of the two morphotypes. Similar
438 to previous studies that have examined possible morphotypes within *M. cavernosa* [25,42,50],
439 the findings of this study indicated the presence of smaller-polyped colonies across a wide depth
440 range and extended the identification of a depth-generalist morphotype into mesophotic depths.
441 This dichotomous variation in *M. cavernosa* morphotypes within sites was primarily
442 observed at West and East FGB, where individuals of the depth-generalist morphotype were
443 found in both depth zones. Shallow-only morphotypes were limited to the coral reef caps from
444 17–20 m, but it is important to note that there is no reef habitat shallower than 17 m at either
445 FGB site. There also appeared to be a potential spatial component affecting morphotype
446 distribution. Samples collected from shallow depth zones of the bank margins were all depth-
447 generalists, while the majority of the samples collected near the center of the bank caps were
448 shallow-only. While collections at shallow depths within West and East FGB were only ~165-
449 420 m apart, it is possible that local environmental conditions between marginal and mid-bank
450 habitats may have resulted in selection towards one morphotype over another. In particular,
451 current patterns on the margins may support increased upwelling of zooplankton [39,40],
452 possibly leading to an advantage for the smaller depth-generalist morphotype, but data regarding
453 fine-scale current dynamics and food availability are lacking for the Flower Garden Banks.
454 The exclusion of shallow-only morphotypes from mesophotic sites was consistent across
455 other sites in the NW GOM; *M. cavernosa* populations at Bright (50 m) and McGrail (50 m)
456 Banks were comprised almost exclusively of depth-generalist morphotypes (Fig 3). However,

457 this pattern did not hold in the SE GOM, as most mesophotic *M. cavernosa* at Pulley Ridge were
458 identified as the shallow-only morphotype based primarily on corallite spacing. Other
459 characteristics beyond corallite spacing, however, suggested that *M. cavernosa* at Pulley Ridge
460 may represent a hybrid of depth-generalist and shallow-only morphotypes. Colonies within
461 Pulley Ridge exhibited significant deviation in corallite structure (notably corallite diameter,
462 theca height, and corallite height) from the shallow-only morphotype. Variations of corallite size
463 and height were indicative of differences seen across shallow and mesophotic depths elsewhere
464 in the GOM and likely represent skeletal adaptation among the mesophotic corals at Pulley
465 Ridge better suited to low-light environments.

466 Light is considered to be one of the dominant environmental drivers of coral morphology
467 [20,21] and distinct separation of morphotype distribution has been observed in some studies
468 [8,10,42], though not in others [50,83]. The occurrence of both depth-generalist and shallow-
469 only colonies in the shallow depth zone at both FGB sites suggests that light or local
470 environments are not the only factors influencing corallite morphology and therefore phenotypic
471 plasticity may not be the dominant driver of coral morphology in this region [20,50]. Based on
472 the variable presence of the two observed morphotypes within the GOM, we hypothesize that
473 genotypic differences in *M. cavernosa* may be contributing to the observed distribution of
474 morphotypes. This hypothesis is contingent on many factors, including the ability of depth-
475 generalist genotypes to spread and survive in other environments beyond their source
476 populations. Such a pattern appears to be the case for mesophotic habitats within the GOM [69],
477 while coral larval characteristics also support such a dispersal pattern, as lipid-rich larvae tend to
478 float from deeper to shallower water [84,85].

Potential genotypic influence on morphotype

The comparison of genetic structure within the FGB determined that morphotype, regardless of assignment method, had a small but significant effect on population differentiation. Despite evidence that morphotypes were significantly differentiated, however, the structure analysis predicted population panmixia (see also [69]). It appears that the slight differentiation is the result of genotypic differences between morphotypes, although there was no evidence to suggest the presence of cryptic speciation or a lack of gene flow between morphotypes. However, it must be noted that microsatellites may not be as sensitive to detecting cryptic morphotypes as nuclear markers such as *ß-tubulin* [50,86] or identifying selection as single nucleotide polymorphisms (SNPs) [87]. Results from previous population genetics studies suggest that there is a high degree of polymorphism within *M. cavernosa* populations across the Tropical Western Atlantic through ecological timescales [50,83]. Polymorphism within this species has led to the identification of multiple morphotypes in the absence of reproductive isolation or adaptive radiation. The lack of strong genetic isolation observed across this species' range is quite interesting and is yet unexplained by differences due to environmental or genetic factors alone. Polymorphic differences may represent physiological tradeoffs among shallow and mesophotic conspecifics pertaining to differences in feeding strategy, calcification, optical properties and light capture, symbiont communities, and perhaps even stress resilience [9,25,33,82], although research to establish a link between morphotypes and potential physiological advantages is currently limited. The depth-generalist morphotype had skeletal characteristics that likely contribute to enhanced light capture at mesophotic depths through increased light scatter within the skeleton, including taller corallites and longer septa. The depth-generalist morphotype also had higher symbiont densities and chlorophyll concentrations that

502 may support increased light capture (Fig 7) [25]. Corallite characteristics and increased symbiont
503 densities were retained in the depth-generalist morphotype even at shallow depths, suggesting
504 aspects of the symbiosis other than light availability control the abundance of algal cells and
505 chlorophyll content.

506 Under light-limited conditions, increased light scattering and symbiont densities are
507 advantageous and likely confer enhanced photosynthesis and possibly faster growth rates [80].
508 During high light conditions leading to thermal stress, however, increased light amplification can
509 result in more severe bleaching responses [88]. As symbiont density is reduced through
510 bleaching, the effect of light scattering increases and creates a positive feedback loop, exposing
511 additional symbionts to high intensities of light [82]. As a result, corals with higher light
512 scattering skeletal properties may confer lower bleaching resistance and be therefore less suited
513 to higher light environments. Bleaching events due to excess solar radiation may be more likely
514 in shallow reef habitats as compared to mesophotic habitats [26]. We hypothesize that the depth-
515 generalist morphotype may be therefore less abundant at shallow depths in the Flower Garden
516 Banks due in part to lower bleaching resistance.

517 To explain the sole presence of the shallow-only morphotype at both mesophotic Pulley
518 Ridge and shallow Dry Tortugas, we must also consider genetic variation beyond that attributed
519 to morphological differences. Given the patterns of morphotype depth distribution in the NW
520 GOM, Pulley Ridge would be expected to be comprised of primarily the depth-generalist
521 morphotype and Dry Tortugas would be expected to include a mixed population of both
522 morphotypes. The relative lack of the depth-generalist morphotype observed at both sites may
523 have instead resulted from low larval dispersal and population connectivity in the SE GOM.
524 Population genetics analyses suggest a relative isolation of Pulley Ridge *M. cavernosa* from

525 other sites in the GOM and TWA [47,69] and assessments of coral community structure show a
526 recent, sharp decline in coral abundance on Pulley Ridge [58,59]. It is possible that Pulley Ridge
527 and Dry Tortugas were initially colonized by the shallow-only morphotype, or alternatively, both
528 morphotypes have been recruited but environmental conditions in the region favor corals with
529 corallite spacing similar to the shallow-only morphotype. The former seems more likely given
530 the relative isolation of the SE GOM and the small population size of *M. cavernosa* at Pulley
531 Ridge estimated from migration models and surveys [58,59,69]. Divergence from the shallow-
532 only morphotype at Pulley Ridge toward a hybrid morphotype may have then been the result of
533 photoadaptation towards smaller corallites at mesophotic depths.

534 Throughout the fossil record for the past 25 million years, *M. cavernosa* populations in
535 other regions of the TWA have demonstrated remarkable and persistent morphological variation
536 that has not been attributed to any distinct genetic lineages [50,83]. The ability of multiple
537 morphotypes to be maintained in absence of selection, reproductive isolation, or cryptic
538 speciation may be due in part to high genetic diversity across much of this species' range [89].
539 Therefore, a combination of both environmental and genotypic factors likely drives
540 morphological plasticity. The patterns of low genetic diversity observed in the SE GOM support
541 the observed lack of the depth-generalist morphotype in this region, despite Pulley Ridge being
542 the deepest site examined in this study. This observation reinforces the notion that morphological
543 variation among *M. cavernosa* represents a combination of genotypic variation and phenotypic
544 plasticity rather than responses to environmental stimuli alone. Further examination into the
545 relationship between coral genotype and morphotype is required to understand differences
546 among shallow and mesophotic coral populations across the GOM. Assessments of skeletal
547 optical properties are also recommended to determine whether morphotypes in *M. cavernosa*

548 confer physiological and resilience tradeoffs. Lastly, complementary analyses of morphological
549 variation, metabolic physiology, and environmental conditions can allow investigation into the
550 relative roles of photosynthesis and heterotrophy in mesophotic environments [33,41]. A better
551 understanding of morphological variation within coral species may uncover how physiology
552 varies across individuals and how depth-generalist species can be successful in a variety of reef
553 habitats.

Acknowledgements

We acknowledge the staff of Flower Garden Banks and Florida Keys National Marine Sanctuaries; crews of the R/V *Manta* and M/V *Spree*; and L. Horn and J. White from the University of North Carolina at Wilmington Undersea Vehicle Program for assistance with sample collection and permits. J. Beal, J. Emmert, R. Susen, C. Ledford, J. Polinski, A. Alker, D. Dodge, P. Gardner, M. McCallister, M. Ajemian, R. Christian, and M. Dickson provided diving support. Special thanks to J. Polinski, D. Perez, H. Clinton, P. Gardner, and D. Dodge for providing the algal symbiont and chlorophyll data, and to A. Alker for assisting with the morphometrics data collection. This research was funded by the NOAA Office of Ocean Exploration and Research under awards NA09OAR4320073 and NA14OAR4320260 to the Cooperative Institute for Ocean Exploration, Research and Technology (CIOERT) at Florida Atlantic University's (FAU) Harbor Branch Oceanographic Institute (HBOI) and the NOAA National Centers for Coastal Ocean Science under award NA11NOS4780045 to the Cooperative Institute for Marine and Atmospheric Studies (CIMAS) at the University of Miami. Additional funding was provided by the Banbury Foundation through the Robertson Coral Reef Research and Conservation Program at HBOI, and by graduate student fellowships/grants from FAU. This is contribution number XXXX from Harbor Branch Oceanographic Institute at FAU.

Data reporting

All protocols included in this study can be found in a GitHub repository at https://github.com/mstudiva/Mcav-morphometrics. Datasets generated for this study can be found in a Dryad repository XXXX.

References

1. Paz-García DA, Hellberg ME, García-de-León FJ, Balart EF. Switch between morphospecies of *Pocillopora* corals. The American Naturalist. 2015;186: 434–440. doi:10.1086/682363
2. Amaral FD. Morphological variation in the reef coral *Montastrea cavernosa* in Brazil. Coral Reefs. Springer-Verlag; 1994;13: 113–117. doi:10.1007/BF00300771
3. Menezes N, Neves E, Kikuchi RKP, Johnsson R. Morphological variation in the Atlantic genus *Siderastrea* (Anthozoa, Scleractinia). Papéis Avulsos de Zoologia (São Paulo). 2014;54: 199–208. doi:10.1590/0031-1049.2014.54.16
4. Rocha RJM, Silva AMB, Fernandes MHV, Cruz ICS, Rosa R, Calado R. Contrasting light spectra constrain the macro and microstructures of scleractinian corals. PLOS ONE. 2014;9: e105863. doi:10.1371/journal.pone.0105863
5. Budd AF, Fukami H, Smith ND, Knowlton N. Taxonomic classification of the reef coral family Mussidae (Cnidaria: Anthozoa: Scleractinia). Zoological Journal of the Linnean Society. 2012;166: 465–529. doi:10.1111/j.1096-3642.2012.00855.x
6. Soto D, De Palmas S, Ho MJ, Denis V, Chen CA. Spatial variation in the morphological traits of *Pocillopora verrucosa* along a depth gradient in Taiwan. PLOS ONE; 2018;13: e0202586. doi:10.1371/journal.pone.0202586
7. Wirshing HH, Baker AC. Molecular evolution of calcification genes in morphologically similar but phylogenetically unrelated scleractinian corals. Molecular Phylogenetics and Evolution. Elsevier Inc.; 2014;77: 281–295. doi:10.1016/j.ympev.2014.04.015
8. Pandolfi JM, Budd AF. Morphology and ecological zonation of Caribbean reef corals: The *Montastraea "annularis"* species complex. Marine Ecology Progress Series. 2008;369:

599 89–102. doi:10.3354/meps07570

600 9. Klaus JS, Budd AF, Heikoop JM, Fouke BW. Environmental controls on corallite
601 morphology in the reef coral *Montastraea annularis*. Bulletin of Marine Science. 2007;80:
602 233–260.

603 10. Weil E, Knowton N. A multi-character analysis of the Caribbean coral *Montastraea*
604 *annularis* (Ellis and Solander, 1786) and its two sibling species, *M. faveolata* (Ellis and
605 Solander, 1786) and *M. franksi* (Gregory, 1895). Bulletin of Marine Science. 1994;55:
606 151–175.

607 11. Willis BL, Ayre DJ. Asexual reproduction and genetic determination of growth form in
608 the coral *Pavona cactus*: biochemical genetic and immunogenic evidence. Oecologia.
609 1985;65: 516–525.

610 12. Foster AB. Phenotypic plasticity in the reef corals *Montastraea annularis* (Ellis &
611 Solander) and *Siderastrea siderea* (Ellis & Solander). Journal of Experimental Marine
612 Biology and Ecology. 1979;39: 25–54. doi:10.1016/0022-0981(79)90003-0

613 13. Via S, Lande R. Genotype-environment interaction and the evolution of phenotypic
614 plasticity. Evolution. 1985;39: 505–522.

615 14. Barshis DJ, Stillman JH, Gates RD, Toonen RJ, Smith LW, Birkeland C. Protein
616 expression and genetic structure of the coral *Porites lobata* in an environmentally extreme
617 Samoan back reef: does host genotype limit phenotypic plasticity? Molecular Ecology.
618 2010;19: 1705–1720. doi:10.1111/j.1365-294X.2010.04574.x

619 15. Bruno JF, Edmunds PJ. Clonal variation for phenotypic plasticity in the coral *Madracis*
620 *mirabilis*. Ecology. 1997;78: 2177–2190. doi:10.1890/0012-
621 9658(1997)078[2177:CVFPPI]2.0.CO;2

16. Todd PA, Ladle RJ, Lewin-Koh NJI, Chou LM. Genotype x environment interactions in transplanted clones of the massive corals *Favia speciosa* and *Diploastrea heliopora*. Marine Ecology Progress Series. 2004;271: 167–182.

17. Budd AF. Variation within coral colonies and its importance for interpreting fossil species. Journal of Paleontology. 1985;59: 1359–1381. doi:10.2307/1304950

18. Ayre DJ, Hughes TP. Genotypic diversity and gene flow in brooding and spawning corals along the Great Barrier Reef, Australia. Evolution. 2000;54: 1590–1605. doi:10.1111/j.0014-3820.2000.tb00704.x

19. Benzie JAH. Genetic structure of coral reef organisms: ghosts of dispersal past. American Zoologist. 1999;39: 131–145. doi:10.1093/icb/39.1.131

20. Todd PA. Morphological plasticity in scleractinian corals. Biological Reviews. 2008;83: 315–337. doi:10.1111/j.1469-185X.2008.00045.x

21. Beltrán-Torres AU, Carricart-Ganivet JP. Skeletal morphological variation in *Montastraea cavernosa* (Cnidaria: Scleractinia) at Isla Verde Coral Reef, Veracruz, Mexico. Revista de Biologia Tropical. 1993;41: 559–562.

22. Graus RR, Macintyre IG. Variation in growth forms of the reef coral *Montastrea annularis* (Ellis and Solander): a quantitative evaluation of growth response to light distribution using computer simulation. Smithsonian Contributions to the Marine Sciences. 1982;12: 441–464.

23. Gleason DF. The control and adaptive significance of morphological variation in the reef coral *Porites asteroides*. Ph.D. Thesis, University of Houston. 1992.

24. Dustan P. Distribution of zooxanthellae and photosynthetic chloroplast pigments of the reef-building coral *Montastraea annularis* (Ellis and Solander) in relation to depth on a

West Indian coral reef. Bulletin of Marine Science. 1979;29: 79–95.

25. Lasker HR. Phenotypic variation in the coral *Montastrea cavernosa* and its effects on colony energetics. The Biological Bulletin. 1981;160: 292–302.

26. Lesser MP, Slattery M, Leichter JJ. Ecology of mesophotic coral reefs. Journal of Experimental Marine Biology and Ecology. 2009;375: 1–8. doi:10.1016/j.jembe.2009.05.009

27. Falkowski PG, Jokiel PL, Kinzie RA. Irradiance and corals. Ecosystems of the world. 1990;25: 89–107.

28. Leichter JJ, Wing SR, Miller SL, Denny MW. Pulsed delivery of subthermocline water to Conch Reef (Florida Keys) by internal tidal bores. Limnology and Oceanography. 1996;41: 1490–1501. doi:10.4319/lo.1996.41.7.1490

29. Reed JK. Comparison of deep-water coral reefs and lithoherms off southeastern USA. Hydrobiologia. 2002;471: 57–69. doi:10.1023/A:1016593018389

30. West JM, Harvell CD, Walls AM. Morphological plasticity in a gorgonian coral (*Briareum asbestinum*) over a depth cline. Marine Ecology Progress Series. 1993;94: 61–69. doi:10.3354/meps094061

31. Ow YX, Todd PA. Light-induced morphological plasticity in the scleractinian coral *Goniastrea pectinata* and its functional significance. Coral Reefs. 2010;29: 797–808. doi:10.1007/s00338-010-0631-4

32. Porter JW. Autotrophy, heterotrophy, and resource partitioning in Caribbean reef-building corals. The American Naturalist. 1976;110: 731–742.

33. Lesser MP, Slattery M, Stat M, Ojimi M, Gates RD, Grottoli A. Photoacclimatization by the coral *Montastraea cavernosa* in the mesophotic zone: light, food, and genetics.

Ecology. 2010;91: 990–1003. doi:10.1890/09-0313.1

34. Slattery M, Lesser MP, Brazeau DA, Stokes MD, Leichter JJ. Connectivity and stability of mesophotic coral reefs. Journal of Experimental Marine Biology and Ecology. 2011;408: 32–41. doi:10.1016/j.jembe.2011.07.024

35. Bongaerts P, Ridgway T, Sampayo EM, Hoegh-Guldberg O. Assessing the 'deep reef refugia' hypothesis: focus on Caribbean reefs. Coral Reefs. 2010;29: 309–327. doi:10.1007/s00338-009-0581-x

36. Muscatine L, Porter JW, Kaplan IR. Resource partitioning by reef corals as determined from stable isotope composition. I. δ13N of zooxanthellae and animal tissue versus depth. Marine Biology. 1989;100: 185–193. doi:10.1007/BF00391957

37. Muscatine L, Kaplan IR. Resource partitioning by reef corals as determined from stable isotope composition. II. δ15N of zooxanthellae and animal tissue versus depth. Pacific Science. 1994;48: 304–312. doi:10.1007/BF00391957

38. Lesser MP, Slattery M. Ecology of Caribbean sponges: are top-down or bottom-up processes more important? PLOS ONE. 2013;8: e79799. doi:10.1371/journal.pone.0079799

39. Leichter JJ, Genovese SJ. Intermittent upwelling and subsidized growth of the scleractinian coral *Madracis mirabilis* on the deep fore-reef slope of Discovery Bay, Jamaica. Marine Ecology Progress Series. 2006;316: 95–103.

40. Leichter JJ, Paytan A, Wankel S, Hanson K, Miller S, Altabet MA. Nitrogen and oxygen isotopic signatures of subsurface nitrate seaward of the Florida Keys reef tract. Limnology and Oceanography. 2007;52: 1258–1267. doi:10.4319/lo.2007.52.3.1258

41. Lesser MP, Mazel C, Phinney D, Yentsch CS. Light absorption and utilization by colonies

of the congeneric hermatypic corals *Montastraea faveolata* and *Montastraea cavernosa*. Limnology and Oceanography. 2000;45: 76–86. doi:10.4319/lo.2000.45.1.0076

42. Ruiz Torres H. Morphometric examination of corallite and colony variability in the Caribbean coral *Montastraea cavernosa*. M.Sc. Thesis, University of Puerto Rico, Mayagüez. 2004.

43. Sebens KP. Adaptive responses to water flow: morphology, energetics, and distribution of reef corals. Proceedings of the 8th International Coral Reef Symposium, Panama City, Panama. 1997;2: 1053–1058.

44. Puglise KA, Hinderstein LM, Marr J, Dowgiallo MJ, Martinez FA. Mesophotic coral ecosystems research strategy: international workshop to prioritize research and management needs for mesophotic coral ecosystems, Jupiter, Florida, 12-15 July 2008. NOAA National Centers for Coastal Ocean Science, Center for Sponsored Coastal Ocean Research, and Office of Ocean Exploration and Research, NOAA Undersea Research Program. NOAA Technical Memorandum NOS NCCOS 98 and OAR OER 2, Silver Spring, MD; 2009.

45. Goodbody-Gringley G, Marchini C, Chequer AD, Goffredo S. Population structure of *Montastraea cavernosa* on shallow versus mesophotic reefs in Bermuda. PLOS ONE. 2015;10: 1–17. doi:10.1371/journal.pone.0142427

46. Goodbody-Gringley G, Waletich J. Morphological plasticity of the depth generalist coral, *Montastraea cavernosa*, on mesophotic reefs in Bermuda. Ecology. 2018; doi:10.1002/ecy.2232

47. Serrano XM, Baums IB, O'Reilly K, Smith TB, Jones RJ, Shearer TL, et al. Geographic differences in vertical connectivity in the Caribbean coral *Montastraea cavernosa* despite

714 high levels of horizontal connectivity at shallow depths. Molecular Ecology. 2014;23:
715 4226–4240. doi:10.1111/mec.12861
716 48. Kahng SE, Garcia-Sais JR, Spalding HL, Brokovich E, Wagner D, Weil E, et al.
717 Community ecology of mesophotic coral reef ecosystems. Coral Reefs. 2010;29: 255–275.
718 doi:10.1007/s00338-010-0593-6
719 49. Kahng SE, Copus JM, Wagner D. Recent advances in the ecology of mesophotic coral
720 ecosystems (MCEs). Current Opinion in Environmental Sustainability. 2014;7: 72–81.
721 doi:10.1016/j.cosust.2013.11.019
722 50. Budd AF, Nunes FLD, Weil E, Pandolfi JM. Polymorphism in a common Atlantic reef
723 coral (*Montastraea cavernosa*) and its long-term evolutionary implications. Evolutionary
724 Ecology. 2012;26: 265–290. doi:10.1007/s10682-010-9460-8
725 51. Iglesias-Prieto R, Beltrán VH, Lajeunesse TC, Reyes-Bonilla H, Thomé PE. Different
726 algal symbionts explain the vertical distribution of dominant reef corals in the eastern
727 Pacific. Proceedings of the Royal Society B. 2004;271: 1757–1763.
728 doi:10.1098/rspb.2004.2757
729 52. Clark R, Taylor JC, Buckel CA, Kracker LM. Fish and benthic communities of the Flower
730 Garden Banks National Marine Sanctuary: science to support sanctuary management.
731 NOAA Technical Memorandum NOS NCCOS 179, Silver Spring; 2014.
732 53. Hickerson EL, Schmahl GP, Johnston MA, Nuttall MF, Embesi JA, Eckert RJ. Flower
733 Garden Banks – a refuge in the Gulf of Mexico? Proceedings of the 12th International
734 Coral Reef Symposium, Cairns, Australia. 2012;1: 9–13.
735 54. Hickerson EL, Schmahl GP, Robbart M, Precht WF, Caldow C. The state of coral reef
736 ecosystems of the Flower Garden Banks, Stetson Bank, and other banks in the

northwestern Gulf of Mexico. The state of coral reef ecosystems of the United States and Pacific Freely Associated States: 2008. NOAA Technical Memorandum NOS NCCOS, Silver Spring; 2008. pp. 189–217.

55. Schmahl GP, Hickerson EL, Precht WF. Biology and ecology of coral reefs and coral communities in the Flower Garden Banks region, northwestern Gulf of Mexico. In: Riegl BM, Dodge RE, editors. Coral reefs of the USA. Dordrecht: Springer; 2008. pp. 221–261. doi:10.1007/978-1-4020-6847-8_6

56. Voss JD, Williams MA, Reed JK, Clark R. Benthic and fish communities in the mid and lower mesphotic zone of the sanctuary. In: Clark R, Taylor JC, Buckel CA, Kracker LM, editors. Fish and benthic communities of the Flower Garden Banks National Marine Sanctuary: science to support sanctuary management. Silver Spring, MD: NOAA Technical Memorandum NOS NCCOS 179; 2014. pp. 201–260.

57. Jarrett BD, Hine AC, Halley RB, Naar DF, Locker SD, Neumann AC, et al. Strange bedfellows–a deep-water hermatypic coral reef superimposed on a drowned barrier island; southern Pulley Ridge, SW Florida platform margin. Marine Geology. 2005;214: 295–307. doi:10.1016/j.margeo.2004.11.012

58. Reed J, Farrington S, David A, Harter S, Moe H, Horn L, et al. Characterization of mesophotic coral/sponge habitats and fish assemblages in the regions of Pulley Ridge and Tortugas from ROV dives during R/V Walton Smith cruises of 2012 to 2015. NOAA CIOERT, NOAA-NOS-NCCOS, NOAA Office of Ocean Exploration and Research. Harbor Branch Oceanographic Technical Report Number 178, Fort Pierce; 2017.

59. Slattery M, Moore S, Boye L, Whitney S, Woolsey A, Woolsey M. The Pulley Ridge deep reef is not a stable refugia through time. Coral Reefs. 2018;37: 391–396.

doi:10.1007/s00338-018-1664-3

60. Jaap WC. Stony coral (Milleporidae and Scleractinia) communities in the eastern Gulf of Mexico: a synopsis with insights from the Hourglass collections. Bulletin of Marine Science. 2015;91: 207–253. doi:10.5343/bms.2014.1049

61. Schneider CA, Rasband WS, Eliceiri KW. NIH Image to ImageJ: 25 years of image analysis. Nature Methods. 2012;9: 671–675. doi:10.1038/nmeth.2089

62. Abràmoff MD, Magalhães PJ, Ram SJ. Image processing with ImageJ. Biophotonics International. 2004. pp. 36–41. doi:10.1117/1.3589100

63. Ogle D. FSA: fisheries stock analysis. R package version 0.8.17. 2017.

64. Clarke KR, Gorley RN, Somerfield PJ, Warwick RM. Change in marine communities: an approach to statistical analysis and interpretation, 3rd edition. PRIMER-E: Plymouth; 2014.

65. Clarke KR, Gorley RN. PRIMER v7: User manual/tutorial. PRIMER-E: Plymouth; 2016.

66. Polinski JM, Voss JD. Evidence of adaptation to mesophotic depths in the coral-*Symbiodinium* symbiosis at Flower Garden Banks National Marine Sanctuary and McGrail Bank. Coral Reefs. 2018; doi:10.1007/s00338-018-1701-2

67. Polinski J. Coral-algal symbioses in mesophotic *Montastraea cavernosa* in the Gulf of Mexico. M.Sc. Thesis, Florida Atlantic University. 2016.

68. Kassambara A. ggpubr: “ggplot2” based publication ready plots. R package version 0.1.6. 2017.

69. Studivan MS, Voss JD. Population connectivity among shallow and mesophotic *Montastraea cavernosa* corals in the Gulf of Mexico identifies potential for refugia. Coral Reefs. 2018; Forthcoming.

70. Peakall R, Smouse PE. GENALEX 6: genetic analysis in Excel. Population genetic software for teaching and research. Molecular Ecology Notes. 2006;6: 288–295. doi:10.1111/j.1471-8286.2005.01155.x

71. Peakall R, Smouse PE. GenAlEx 6.5: genetic analysis in Excel. Population genetic software for teaching and research–an update. Bioinformatics. 2012;28: 2537–2539. doi:10.1093/bioinformatics/bts460

72. Pritchard JK, Stephens M, Donnelly P. Inference of population structure using multilocus genotype data. Genetics. 2000;155: 945–959. doi:10.1111/j.1471-8286.2007.01758.x

73. Evanno G, Regnaut S, Goudet J. Detecting the number of clusters of individuals using the software STRUCTURE: a simulation study. Molecular Ecology. 2005;14: 2611–2620. doi:10.1111/j.1365-294X.2005.02553.x

74. Earl DA, VonHoldt BM. STRUCTURE HARVESTER: a website and program for visualizing STRUCTURE output and implementing the Evanno method. Conservation Genetics Resources. 2012;4: 359–361. doi:10.1007/s12686-011-9548-7

75. Kaiser P, Schlichter D, Fricke HW. Influence of light on algal symbionts of the deep water coral *Leptoseris fragilis*. Marine Biology. 1993;117: 45–52. doi:10.1007/BF00346424

76. Ziegler M, Roder CM, Büchel C, Voolstra CR. Mesophotic coral depth acclimatization is a function of host-specific symbiont physiology. Frontiers in Marine Science. 2015;2: 4. doi:10.3389/fmars.2015.00004

77. Smith EG, D'Angelo C, Sharon Y, Tchernov D, Wiedenmann J. Acclimatization of symbiotic corals to mesophotic light environments through wavelength transformation by fluorescent protein pigments. Proceedings of the Royal Society B. 2017;284: 20170320. doi:10.1098/rspb.2017.0320

78. Kahng SE, Hochberg EJ, Apprill A, Wagner D, Luck DG, Perez D, et al. Efficient light harvesting in deep-water zooxanthellate corals. Marine Ecology Progress Series. 2012;455: 65–77. doi:10.3354/meps09657

79. Enríquez S, Méndez ER, Iglesias-Prieto R. Multiple scattering on coral skeletons enhances light absorption by symbiotic algae. Limnology and Oceanography. 2005;50: 1025–1032. doi:10.4319/lo.2005.50.4.1025

80. Scheufen T, Iglesias-Prieto R, Enríquez S. Changes in the number of symbionts and *Symbiodinium* cell pigmentation modulate differentially coral light absorption and photosynthetic performance. Frontiers in Marine Science. 2017;4: 309. doi:10.3389/fmars.2017.00309

81. Enríquez S, Méndez ER, Hoegh-Guldberg O, Iglesias-Prieto R. Key functional role of the optical properties of coral skeletons in coral ecology and evolution. Proceedings of the Royal Society B. The Royal Society; 2017;284: 20161667. doi:10.1098/rspb.2016.1667

82. Marcelino LA, Westneat MW, Stoyneva V, Henss J, Rogers JD, Radosevich A, et al. Modulation of light-enhancement to symbiotic algae by light-scattering in corals and evolutionary trends in bleaching. PLOS ONE. 2013;8: e61492. doi:10.1371/journal.pone.0061492

83. Goodbody-Gringley G, Woollacott RM, Giribet G. Population structure and connectivity in the Atlantic scleractinian coral *Montastraea cavernosa* (Linnaeus, 1767). Marine Ecology. 2012;33: 32–48. doi:10.1111/j.1439-0485.2011.00452.x

84. Arai T, Kato M, Heyward A, Ikeda Y, Iizuka T, Maruyama T. Lipid composition of positively buoyant coral eggs. Coral Reefs. 1993;12: 71–75.

85. Holstein DM, Paris CB, Vaz AC, Smith TB. Modeling vertical coral connectivity and

829 mesophotic refugia. Coral Reefs. 2015;35: 23–37. doi:10.1007/s00338-015-1339-2

830 86. Nunes FLD, Norris RD, Knowton N. Implications of isolation and low genetic diversity in
831 peripheral populations of an amphi-Atlantic coral. Molecular Ecology. 2009;18: 4283–
832 4297. doi:10.1111/j.1365-294X.2009.04347.x

833 87. Reid NM, Proestou DA, Clark BW, Warren WC, Colbourne JK, Shaw JR, et al. The
834 genomic landscape of rapid repeated evolutionary adaptation to toxic pollution in wild
835 fish. Science. 2016;354: 1305–1308. doi:10.1126/science.aah4993

836 88. Cunning R, Baker AC. Excess algal symbionts increase the susceptibility of reef corals to
837 bleaching. Nature Climate Change. Nature Publishing Group; 2012;3: 259–262.
838 doi:10.1038/nclimate1711

839 89. Gillespie JH. Population genetics: a concise guide. 2nd ed. Baltimore: The Johns Hopkins
840 University Press; 2010.

841

A
T1C
CYCLE
1
2
3
4
CW
CD
L4S
L1S
5 mm
B
5 mm
C
5 mm

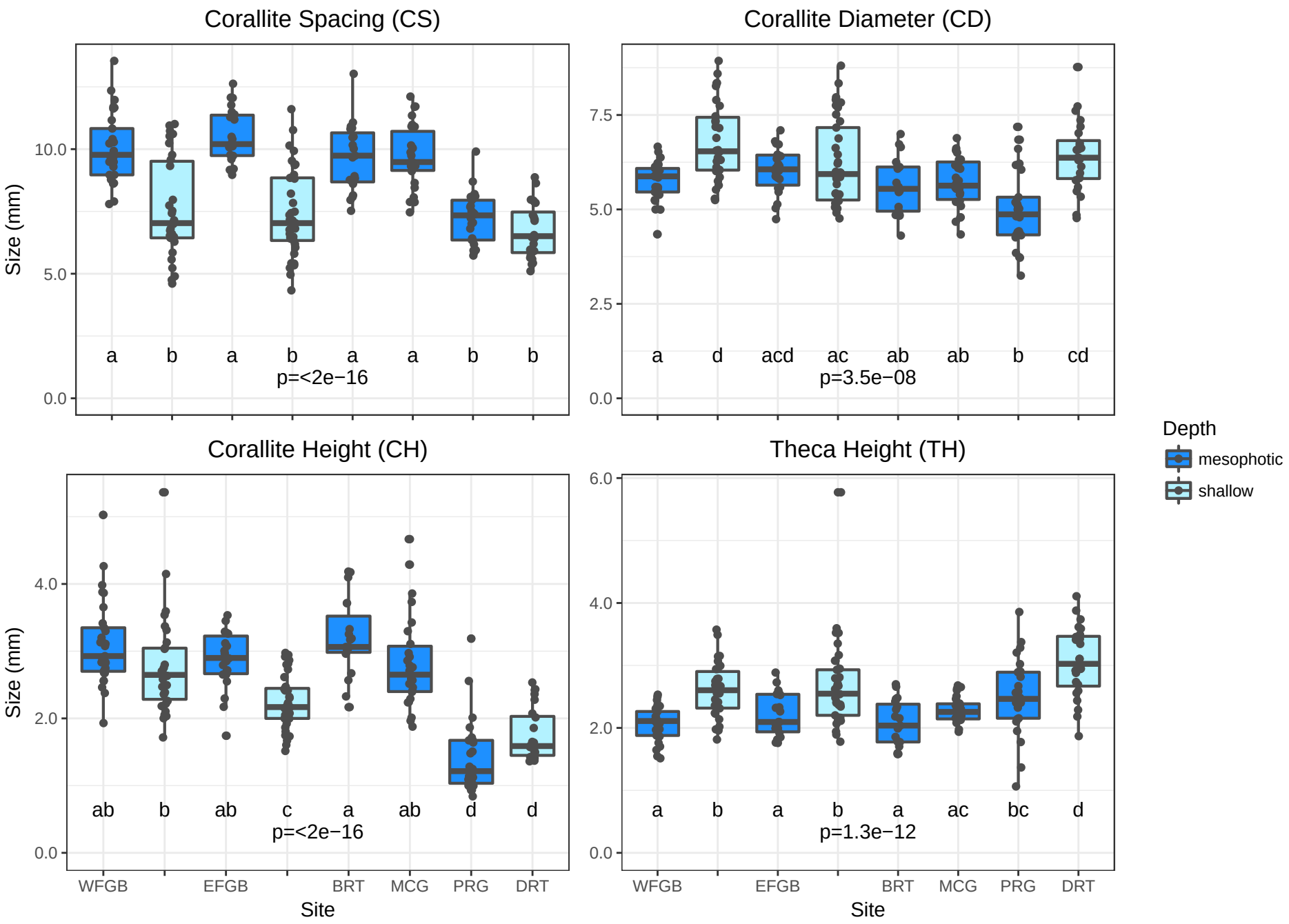
Corallite Spacing (CS)
Corallite Diameter (CD)
Corallite Height (CH)
Theca Height (TH)
Size (mm)
a b a b a a b b
p=<2e−16
a d acd ac ab ab b cd
p=3.5e−08
ab b ab c a ab d d
p=<2e−16
a b a b a ac bc d
p=1.3e−12
WFGB EFGB BRT MCG PRG DRT
Site
Depth
mesophotic
shallow

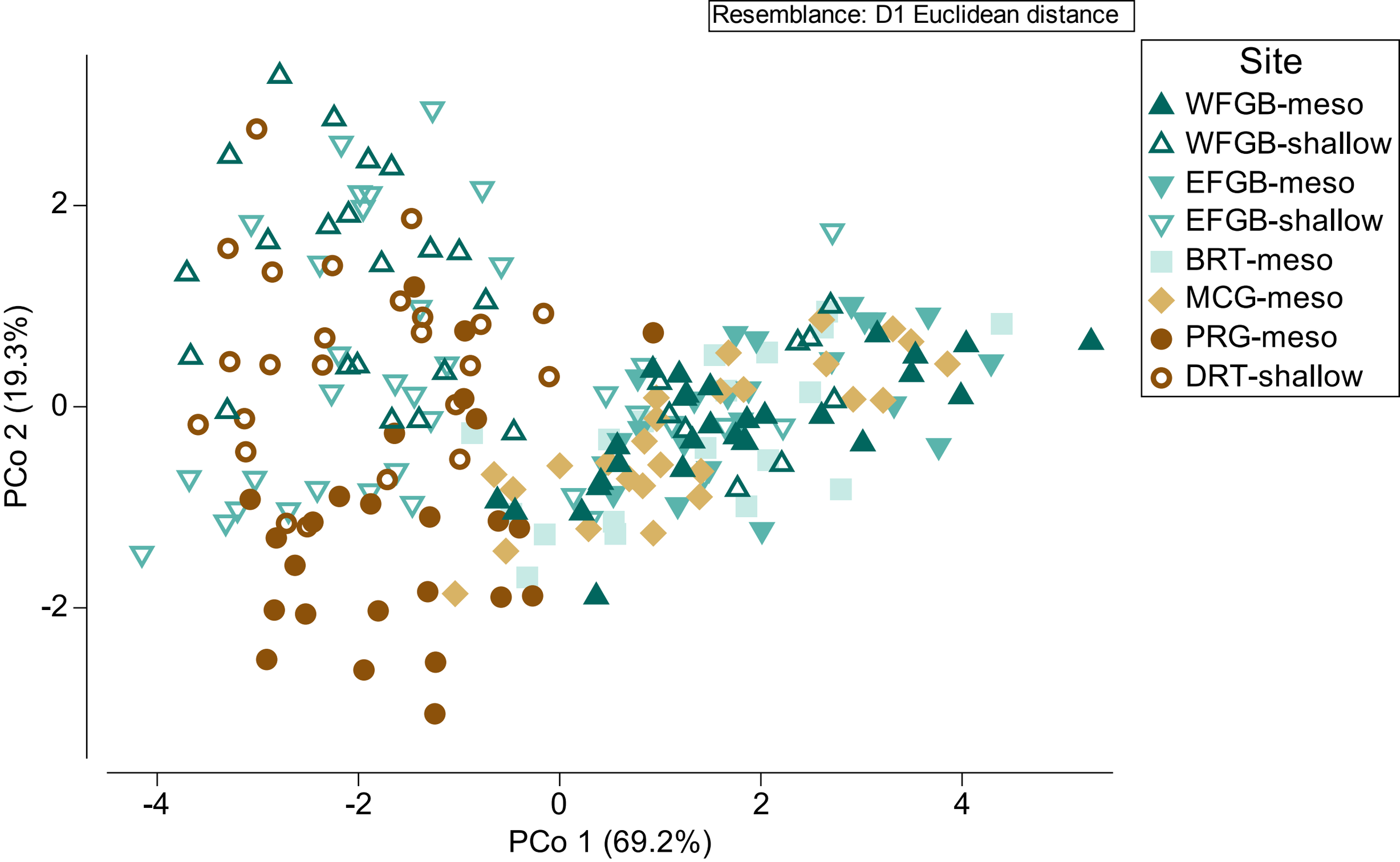
Resemblance: D1 Euclidean distance
Site
WFGB-meso
WFGB-shallow
EFGB-meso
EFGB-shallow
BRT-meso
MCG-meso
PRG-meso
DRT-shallow
PCo 2 (19.3%)
PCo 1 (69.2%)
2
0
-2
-4
-2
0
2
4

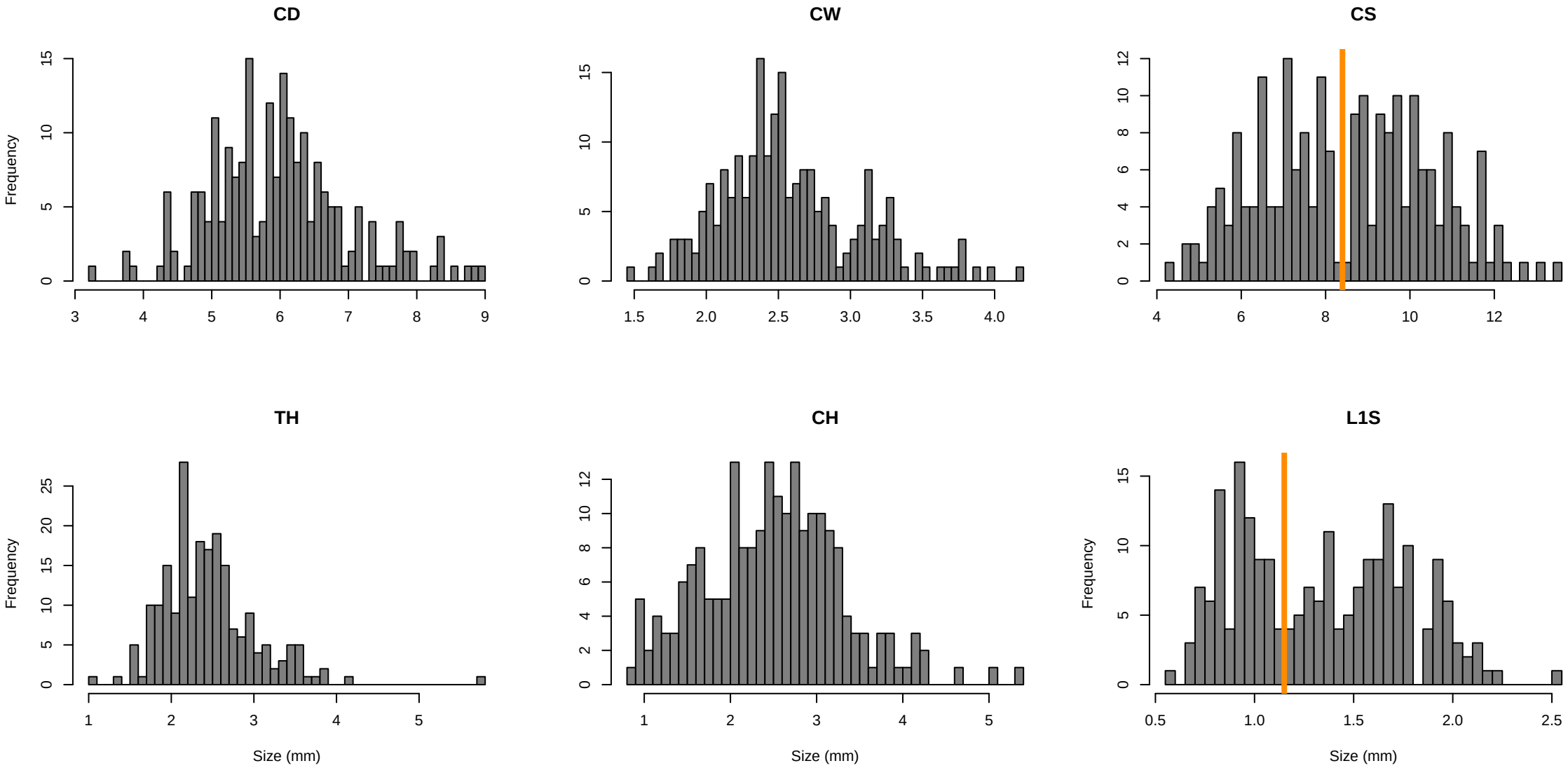
CD
CW
CS
TH
CH
L1S
Frequency
Size (mm)

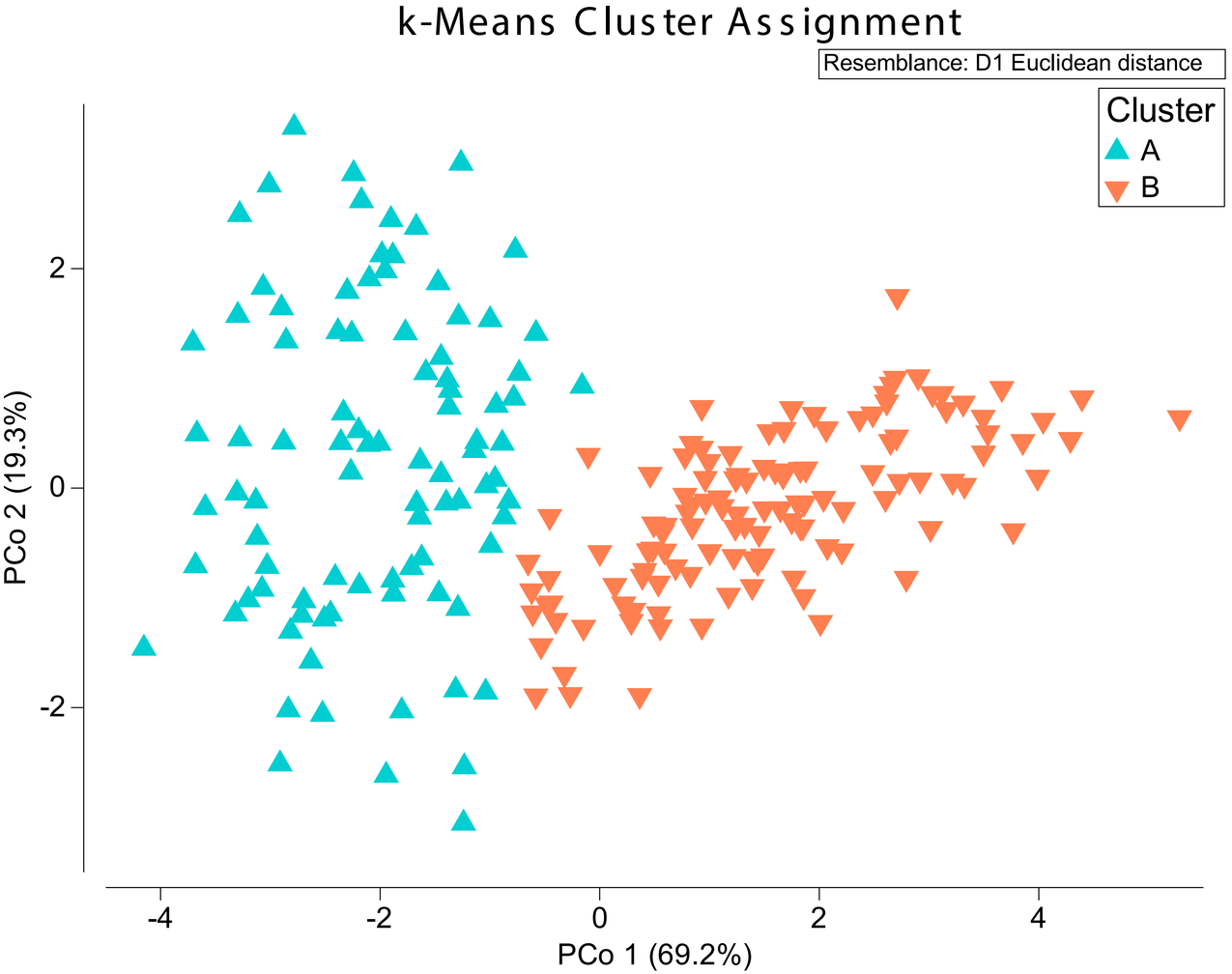
k-Means Cluster Assignment
Resemblance: D1 Euclidean distance
Cluster
A
B
PCo 2 (19.3%)
PCo 1 (69.2%)
2
0
-2
-4
-2
0
2
4

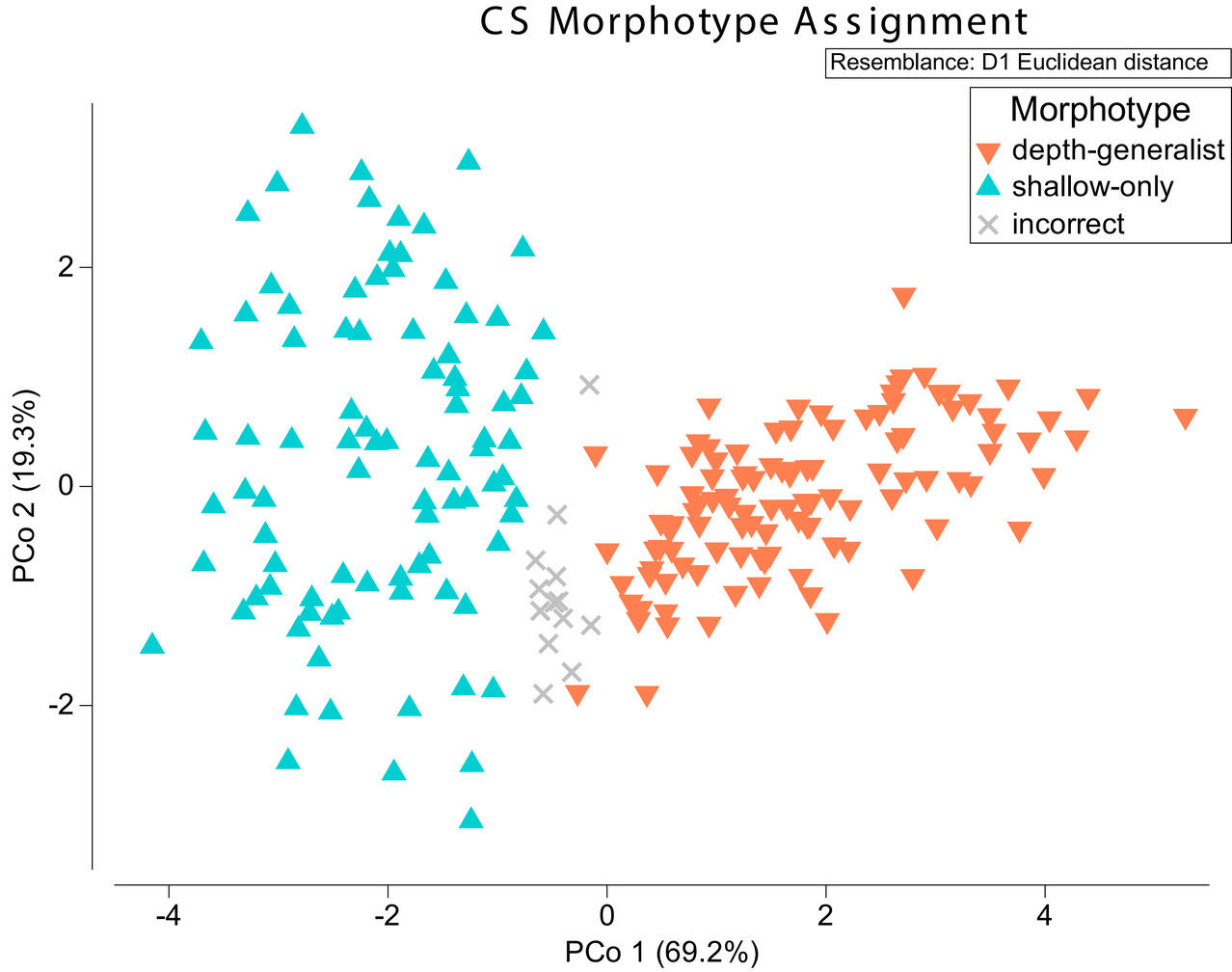
CS Morphotype Assignment
Resemblance: D1 Euclidean distance
Morphotype
depth-generalist
shallow-only
incorrect
PCo 2 (19.3%)
PCo 1 (69.2%)
2
0
-2
-4
-2
0
2
4

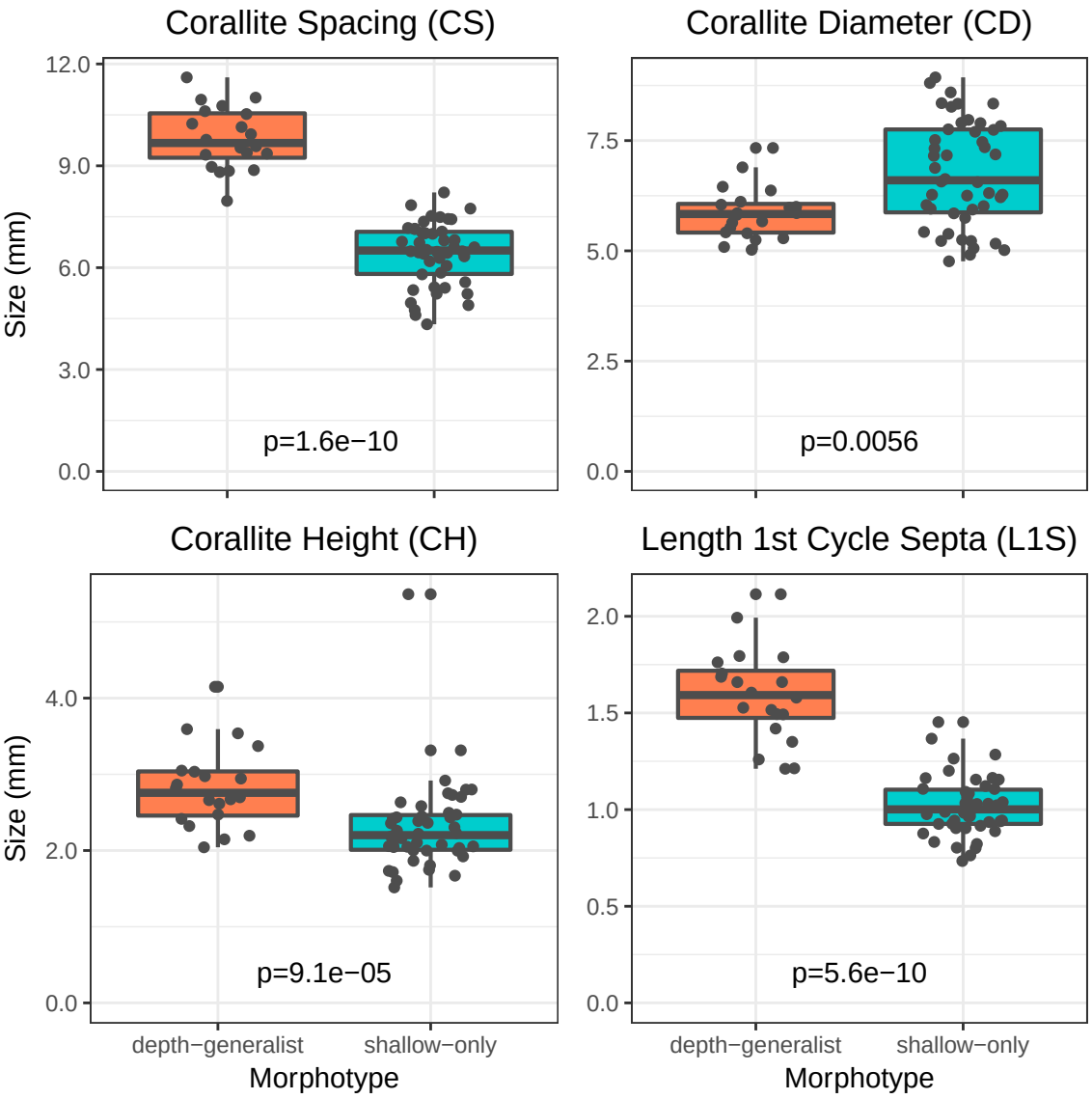
Corallite Spacing (CS)
Corallite Diameter (CD)
Corallite Height (CH)
Length 1st Cycle Septa (L1S)
Size (mm)
12.0
9.0
6.0
3.0
0.0
7.5
5.0
2.5
4.0
2.0
1.5
1.0
0.5
p=1.6e−10
p=0.0056
p=9.1e−05
p=5.6e−10
depth−generalist
shallow−only
Morphotype

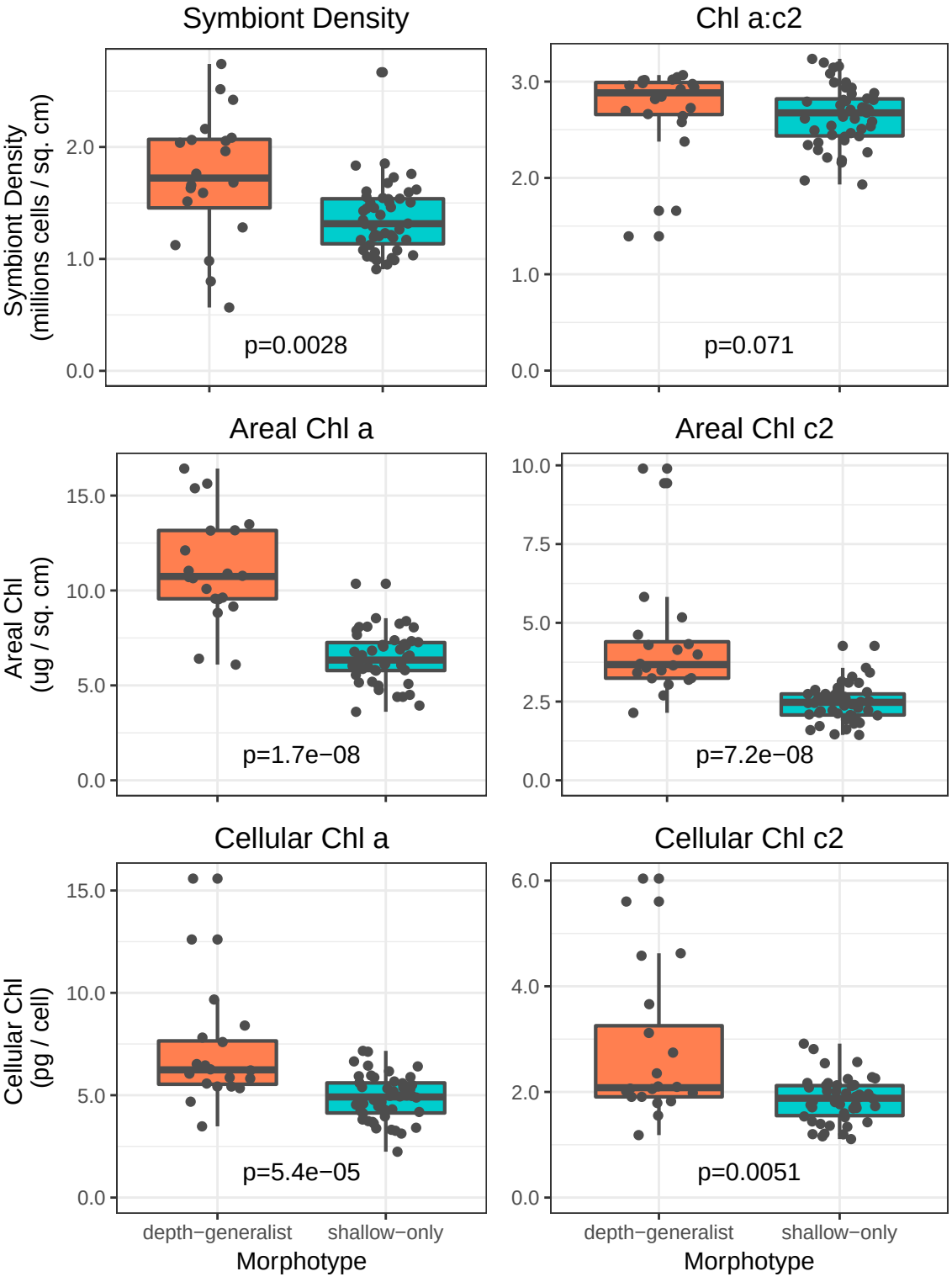
Symbiont Density
Symbiont Density
(millions cells / sq. cm)
2.0
1.0
0.0
p=0.0028
Chl a:c2
3.0
2.0
1.0
0.0
p=0.071
Areal Chl a
Areal Chl
(ug / sq. cm)
15.0
10.0
5.0
0.0
p=1.7e−08
Areal Chl c2
10.0
7.5
5.0
2.5
0.0
p=7.2e−08
Cellular Chl a
Cellular Chl
(pg / cell)
15.0
10.0
5.0
0.0
p=5.4e−05
Cellular Chl c2
6.0
4.0
2.0
0.0
p=0.0051
depth−generalist
shallow−only
Morphotype
depth−generalist
shallow−only
Morphotype